

# Study of first orbit losses of 1 MeV tritons using the Lorentz orbit code in the LHD

journal or publication title	Plasma Science and Technology
volume	21
number	2
page range	025102
year	2019-01-11
URL	<a href="http://hdl.handle.net/10655/00012563">http://hdl.handle.net/10655/00012563</a>

doi: 10.1088/2058-6272/aaeba8



1                   **Study of first orbit losses of 1 MeV tritons using the**

2                                   **Lorentz orbit code in the LHD**

3  
4   Kunihiro OGAWA<sup>1,2</sup>, Mitsutaka ISOBE<sup>1,2</sup>, Takeo NISHITANI<sup>1</sup>, Sadayoshi  
5   MURAKAMI<sup>3</sup>, Ryosuke SEKI<sup>1,2</sup>, Hideo NUGA<sup>1</sup>, Neng PU<sup>2</sup>, Masaki OSAKABE<sup>1,2</sup>, and  
6   LHD Experiment Group<sup>1</sup>

7  
8   1 National Institute for Fusion Science, National Institutes of Natural Sciences, Toki-city,  
9   Gifu, 509-5202, Japan

10   2 SOKENDAI (The Graduate University for Advanced Studies), Toki-city, Gifu, 509-  
11   5202, Japan

12   3 Kyoto University Kyoto-city, Kyoto, 615-8520, Japan

13  
14   Email: kogawa@nifs.ac.jp

15  
16   **Abstract**

17   Shot-integrated measurement of the triton burnup ratio has been performed in the Large  
18   Helical Device (LHD). It was reported that the triton burnup ratio, defined as total DT

19 neutron yield divided by total DD neutron yield, increases significantly in inward shifted  
20 configurations. To understand the magnetic configuration dependence of the triton burnup  
21 ratio, the first orbit loss fraction of 1 MeV tritons is evaluated by means of the Lorentz  
22 orbit code for various magnetic configurations. The first orbit loss of 1 MeV tritons is  
23 seen at  $t$  of less than  $10^{-5}$  s and loss points of the triton are concentrated on the side of the  
24 helical coil case where the magnetic field is relatively weak. The significant decrease of  
25 the first-orbit loss fraction by 15% is obtained with the inward shift of the magnetic axis  
26 position from 3.90 m to 3.55 m. It is found that the decrease of first-orbit loss is due to  
27 the reduction of the first orbit loss of transition and helically trapped tritons.

28

29 **Keywords:** large helical device, tritons, energetic ion, first orbit loss, Lorentz orbit code

30 (Some figure may appear in colour only in the online journal)

## 31 **1. Introduction**

32 One of the key issues for sustaining fusion reactions in a burning plasma is how DT fusion  
33 born alpha particles are sufficiently confined. For understanding the alpha particle  
34 confinement property in a burning plasma, it is valuable to understand the confinement  
35 of energetic particles in existing torus fusion devices. Instead of alpha particles, neutral  
36 beam injection and the ion cyclotron range of frequency heating have been employed to

37 study the energetic ion confinement [1]. In deuterium operations, confinement of 1 MeV  
38 tritons created by d(d,p)t reactions is intensively studied as a simulation study of alpha  
39 particle confinement because the Larmor radius and the precession frequency are the  
40 same as those of DT born 3.5 MeV alpha particles [2]. In addition, the velocity  
41 distribution of tritons is isotropic as alpha particles.

42 In tokamaks, study of 1 MeV triton confinement by experiments and numerical  
43 simulations has been intensively performed in the deuterium experiment [3-8]. In  
44 stellarator and heliotron, the study of the confinement property of alpha particles was  
45 performed using the orbit simulation in a fusion-reactor-relevant machine, of which the  
46 plasma volume is 1000 m<sup>3</sup> and the magnetic field strength is 5 T [9, 10]. The birth profile  
47 of alpha particles is proportional to  $n^2T^2$ , where  $n$  and  $T$  represent fuel ion density and  
48 fuel ion temperature, respectively. Therefore, the loss fraction of alpha particles born in  
49 the core region of the plasma was discussed because the alpha particles mainly born in  
50 the core region. It was reported that most of the alpha particles are confined during the  
51 collisional damping time [10]. The triton burnup experiment was initiated in the first  
52 campaign of deuterium operations in March 2017 on the Large Helical Device (LHD)  
53 [11]. This is the first triton burnup experiment in stellarators/helical devices. The triton  
54 burnup experiments are performed in neutral-beam heated deuterium plasmas. In these

55 experiments, neutrons and 1 MeV tritons are mainly created by beam-thermal DD  
56 reactions. 1 MeV tritons created by DD reaction can undergo secondary DT reaction with  
57 the bulk deuteron while they slowed down. The triton burnup ratio defined by the total  
58 DT neutron amount per discharge divided by the total DD neutron amount per discharge  
59 is surveyed [12]. The scintillating fiber (Sci-Fi) detector using a discriminating method  
60 with absolutely calibrated by the neutron activation system is applied for DT neutron  
61 measurement and the neutron flux monitor is utilized for DD neutron measurement. It  
62 was reported that the triton burnup ratio significantly increases in the inward shifted  
63 configuration. In order to understand the significant increase of triton burnup ratio with  
64 the inward shift of the magnetic axis position, it is important to know the triton  
65 confinement properties in each magnetic configuration. When we considered a classical  
66 confinement of tritons, the loss of tritons could be caused due to the collisionless issue  
67 which is a result of the lost orbit, the collisional issue which the particle reaches the loss  
68 cone due to the collision, and the charge exchange with neutral gas. In these experiments,  
69 typical electron temperature  $T_e$  of 3 keV and typical electron density  $n_e$  of  $2 \times 10^{19} \text{ m}^{-3}$ ,  
70 therefore, it needs more than 2 seconds for 1 MeV triton to decrease its energy to 100 keV  
71 [13]. Here, the triton energy of around 100 keV is considered because the DT cross section  
72 has a peak around this energy. The typical charge exchange loss time of tritons is

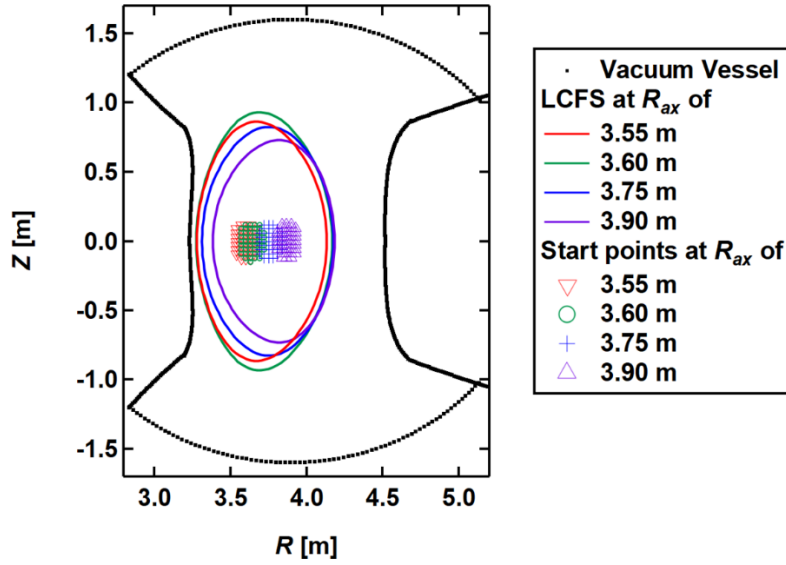
73 evaluated to be 40 ms. Here, neutral density of  $10^{15} \text{ m}^{-3}$  at  $r/a < 0.6$  [14] is used because  
74 tritons mainly exist in the interior region of the plasma. The charge exchange cross section  
75 of  $10^{-20} \text{ m}^2$  at the triton energy of around 100 keV [15] is used. Therefore, the loss of  
76 tritons which occurred in a short period of time,  $t$  of less than 1 ms, is mainly due to the  
77 collisionless issue. In particular, because the Larmor radius of 1 MeV triton evaluated by  
78 energy  $\sim 10$  cm is comparable to the minor radius of the LHD  $\sim 60$  cm, the first orbit loss  
79 could be a considerably large fraction in considering the confinement of 1 MeV tritons.  
80 In this paper, the first-orbit loss fraction of 1 MeV tritons is evaluated as a first step by  
81 means of the Lorentz orbit code in order to understand the magnetic configuration effect  
82 on the triton burnup ratio.

83

## 84 **2. Setup for first orbit loss calculation**

85 The Lorentz orbit following code developed by National Institute for Fusion Science  
86 (LORBIT) [16] is used to evaluate the first-orbit loss fraction of 1 MeV tritons. The code  
87 solves the equation of motion  $m \, d\mathbf{v}/dt = q(\mathbf{E} + \mathbf{v} \times \mathbf{b})$  without including collisions. Here,  $m$ ,  
88  $\mathbf{v}$ ,  $q$ ,  $\mathbf{E}$ , and  $\mathbf{b}$  represent the mass of charged particle, the velocity of charged particle,  
89 charge of the charged particle, the electric field, and the magnetic field, respectively. In  
90 this calculation, we used the magnetic field in a vacuum and assumed no electric field.

91 Note that the effect of the electric field on the 1 MeV triton orbit will be negligibly small  
92 because of the high energy of tritons. We used a random number generator to choose the  
93 radial position, the poloidal angle, the toroidal angle, the velocity component parallel to  
94 the magnetic field and the velocity component perpendicular to the magnetic field. Note  
95 that the normalized minor radius of the birth position of 1 MeV triton is chosen to be less  
96 than 0.2 because most tritons are mainly born in the core region of the plasma. Here, we  
97 choose the simple birth profile of 1 MeV triton in order to exclude plasma parameter  
98 effects to show the magnetic configuration effect on 1 MeV triton confinement clearly.  
99 The initial velocity of the tritons is uniformly distributed in the velocity space with the  
100 Monte Carlo method. In this calculation, we judged that a triton is lost when the triton  
101 reaches the vacuum vessel (VV). Figure 1 shows the poloidal cross section of VV, the last  
102 closed flux surface (LCFS), and birth positions of tritons in the magnetic axis  $R_{ax}$  of 3.55  
103 m, 3.60 m, 3.75 m, and 3.90 m in the vertically elongated poloidal cross section. Note  
104 that the other in-vessel components are not included because the LHD has no limiter and  
105 no ICRF antenna is installed in these experiments. The divertor plate is placed far away  
106 from the plasma, the effect of divertor plates on the first orbit loss ratio of tritons will be  
107 very limited or negligible.



108

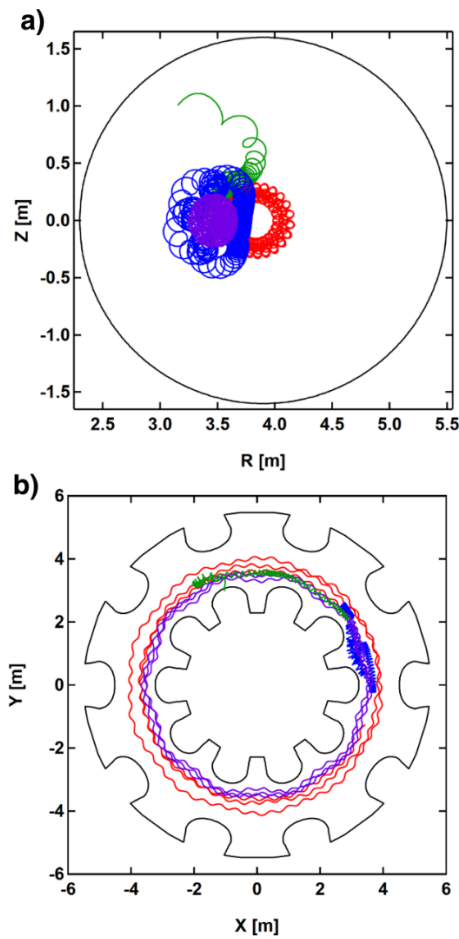
109 Figure 1. The poloidal cross section of the vacuum vessel of the LHD, the LCFS of  $R_{ax}$   
 110 of 3.60 m, 3.75 m, and 3.90 m at the vertical elongated poloidal cross section. Triton birth  
 111 positions located at a normalized minor radius of less than 0.2.

112

113 In the LHD, there are four types of orbits depending on the pitch angle: co-passing transit,  
 114 counter-passing transit, transition, and helically trapped orbits. The orbits of co-passing  
 115 transit and counter-passing transit ions are similar to those in tokamaks, whereas helically  
 116 trapped ions are trapped in a helical ripple created by a pair of twisted helical coils. The  
 117 pitch angles of transition ions correspond to values between those of passing ions and  
 118 those and helically trapped ions. The orbit of the transition particle is unstable and the  
 119 confinement of transition ions is expected to be not good [17]. Typical 1 MeV triton orbits  
 120 in  $R_{ax}/B_t$  of 3.60 m/2.75 T are shown in figure 2. In figure 2, initial pitch angles of co-



121 passing transit, counter-passing transit, transition, and helically trapped tritons are 30  
 122 degrees, 150 degrees, 80 degrees, and 89 degrees, respectively. Here, the start point is set  
 123 to be  $(R, Z, \phi)$  of (3.61 m,  $-0.05$  m, 0 degree) and orbit following time is set to be  $10^{-5}$  s.  
 124 In this case, co-passing transit, counter-passing transit, and helically trapped tritons are  
 125 confined, whereas the transition triton is lost.



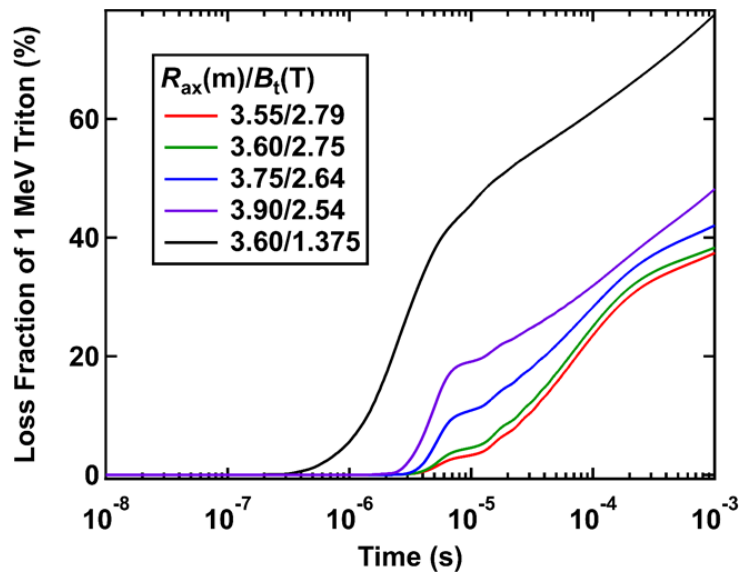
126  
 127 Figure 2. Typical orbit of 1 MeV tritons having the pitch angle of co-passing transit (red),  
 128 transition (green), helically trapped (blue), and counter-passing transit (purple) region a)  
 129 as projected into the  $(R, Z)$  plane and b) as seen from above.

130

### 131 **3. First orbit loss calculation**

132 An orbit following calculation for a relatively long time, around collision time of 1 MeV  
133 tritons, i.e., 1 ms is performed to see the time evolution of the loss fraction of tritons  
134 (figure 3). Here, we launched  $5 \times 10^5$  particles. It is found that the loss fraction becomes  
135 lower with the inward shift of the magnetic axis position in the normal toroidal magnetic  
136 field strength ( $B_t > 2.5$  T). The loss fraction of tritons rapidly increased with  $t$  of from  
137  $2 \times 10^{-6}$  to  $10^{-5}$  s, then became almost flat, and then increased again with time at  $B_t > 2.5$   
138 T. The loss of tritons which occurred at  $t$  less than  $10^{-5}$  s corresponds to the first-orbit loss,  
139 whereas  $t$  greater than  $10^{-5}$  s corresponds to a loss due to collisionless diffusion. Here, the  
140 collisionless diffusion occurs due to the trapping and detrapping of tritons by the magnetic  
141 field ripple. The time trend of the loss fraction is similar to the time trend obtained by the  
142 five dimensional drift kinetic equation solver based on the Boozer coordinates, Global  
143 NEoclassical Transport code (GNET) [18]. Note that the plateau region appears because  
144 it may require time for tritons to reach the VV with the collisionless diffusion. On the  
145 other hand, the loss fraction almost monotonically increases in the half field condition ( $B_t$   
146  $= 1.375$  T). There is almost no plateau region, because the collisionless diffusion of the  
147 tritons is considerably larger due to the lower magnetic field. Figure 4(a) shows the three

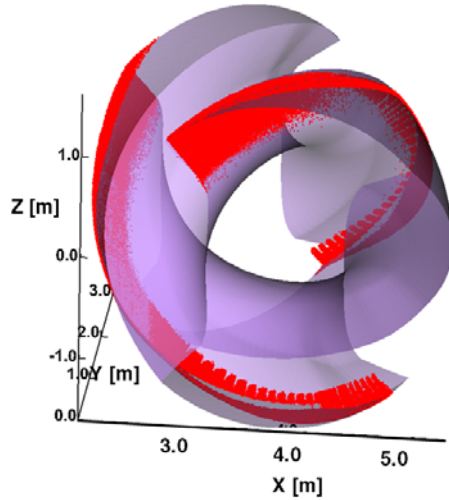
148 dimensional plot of loss points at the toroidal field direction of counter clockwise (CCW)  
 149 from the overhead view at  $R_{ax}/B_t$  of 3.60 m/2.75 T. Here, the orbit following time is set to  
 150 be  $10^{-5}$  s. In this plot, loss points are accumulated in one period of the LHD. The toroidal  
 151 and poloidal angle distribution of lost tritons on the VV is shown in figure 4(b). Here,  
 152 toroidal and poloidal locations of helical coils are indicated in the figure 4(b). Tritons  
 153 reach between the helical coils where magnetic field strength is relatively low, as expected.  
 154 We found that tritons reach one side of the helical coil case and the loss points are changed  
 155 due to the inverted direction of toroidal magnetic field.



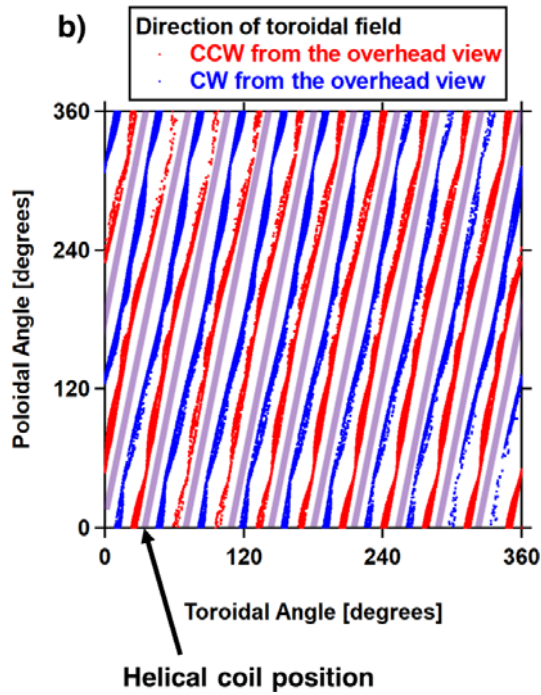
156  
 157 Figure 3. Time evolution of the triton loss fraction. The loss fraction becomes larger with  
 158 the increase of  $R_{ax}$  in the normal  $B_t$  region ( $B_t > 2.5$  T). Significant increase of loss fraction  
 159 is obtained in  $B_t$  of 1.375 T compared with  $B_t$  of 2.75 T in  $R_{ax}$  of 3.60 m.

160

a)  $R_{ax}/B_t = 3.60 \text{ m}/2.75 \text{ T}$   
 Direction of toroidal field is  
 CCW from the overhead view



$R_{ax}/B_t = 3.60 \text{ m}/2.75 \text{ T}$



161

162 Figure 4. Strike points of 1 MeV tritons with three dimensional plot (a) and toroidal and

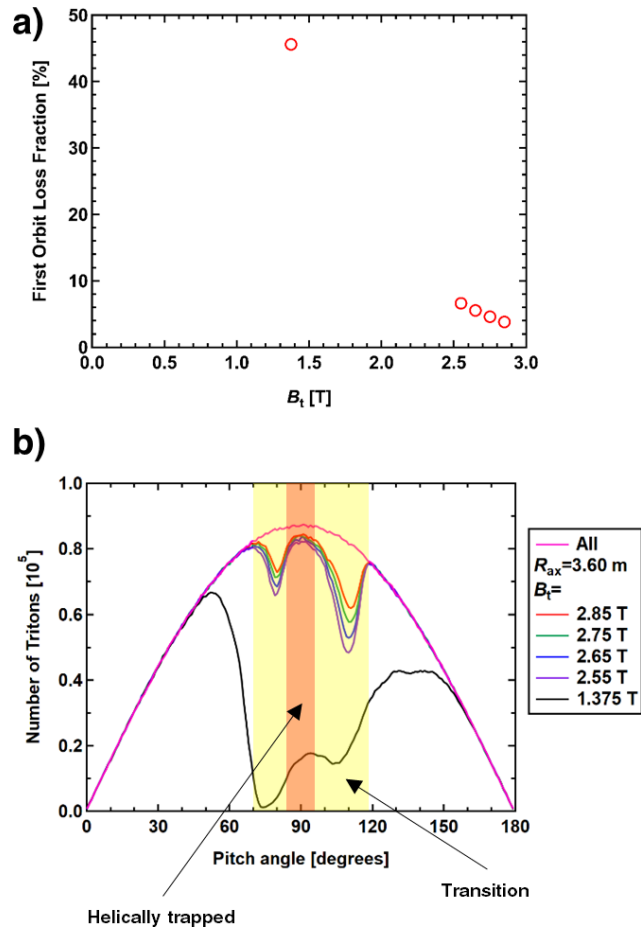
163 poloidal distribution (b). Loss points are located in a relatively narrow region and

164 changed with the reversal of toroidal magnetic field direction.

165

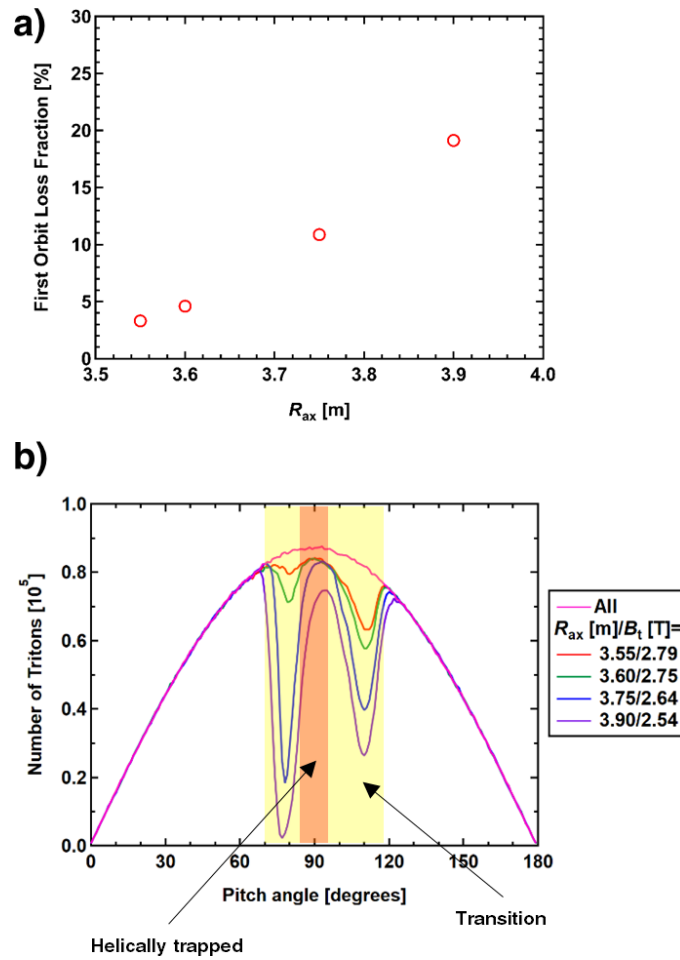
166 As reported in reference [12],  $B_t$  is changed according to the change of  $R_{ax}$  because the  
167 maximum  $B_t$  in each  $R_{ax}$  is decided by the maximum helical coil current in each layer.  
168 Therefore, to clarify  $B_t$  effects on the triton confinement improvement/degradation, an  
169 effect of  $B_t$  on the first orbit loss of 1 MeV tritons is evaluated at  $R_{ax}$  of 3.60 m. In this  
170 calculation,  $10^7$  particles are launched and the orbit following time is set to be  $10^{-5}$  s. The  
171 first orbit loss fraction as a function of  $B_t$  shown in figure 5(a) indicates that the effect of  
172  $B_t$  on the first orbit loss fraction is weak in  $B_t > 2.5$  T. The first orbit loss fractions in  $B_t$   
173 of 2.55 T, 2.65 T, 2.75 T, and 2.85 T are 6.6%, 5.5%, 4.6%, and 3.8%, respectively. Note  
174 that the first orbit loss fraction reaches 46% at the half field strength condition ( $B_t$  of 1.375  
175 T). A pitch angle distribution of tritons launched and confined are shown in Figure 5(b).  
176 Most of the tritons with the exception of some particles having helically trapped and  
177 transition orbits are confined in  $B_t > 2.5$  T. Note that the number of losses in the helically  
178 trapped region is almost unchanged with the change of the magnetic field strength because  
179 the structure of the helical ripple is the same. Hence, the increase of  $B_t$  only provides the  
180 slight improvement of the triton burnup fraction in  $B_t > 2.5$  T. Note that a large fraction  
181 of the first orbit loss of tritons in  $B_t$  of 1.375 T is consistent with the low triton burnup  
182 ratio measured in the experiment [12]. Evaluation of first orbit loss fraction in each  
183 configuration is performed. The number of particles and the orbit following time are the

184 same as the previous calculation. Figure 6(a) shows the first orbit loss fraction of tritons  
185 as a function of  $R_{ax}$ . The loss fraction increases rapidly with outward shift of  $R_{ax}$ . In the  
186 case of the inward shifted configuration, the first orbit loss fraction is around 5%, whereas  
187 the fraction increases around 20% in the outward shifted configuration  $R_{ax}$  of 3.90 m.  
188 Pitch angle distribution of tritons launched and confined is shown in figure 6(b). The  
189 number of confined transition and helically trapped tritons significantly decreased with  
190 the outward shift of  $R_{ax}$ . The loss of helically trapped and transition tritons becomes larger  
191 because the deviation of the orbit from the flux surface becomes larger as the outward  
192 shift of  $R_{ax}$ . The results indicate that decrease of the first orbit loss of tritons is mainly due  
193 to inward shift of  $R_{ax}$  which reduces the first orbit loss of transition and helically-trapped  
194 1 MeV tritons. The decrease of first orbit loss of 1 MeV tritons is one of the important  
195 factors to induce the significant improvement of the triton burnup ratio as the inward shift  
196 of  $R_{ax}$  obtained in the experiment.



197

198 Figure 5. (a) The effect of  $B_t$  on 1 MeV triton loss fraction. The loss fraction is slightly  
 199 changed when  $B_t$  is greater than 2.5 T, whereas there is significantly increase at  $B_t$  of  
 200 1.375 T. (b) Pitch angle distribution of launched 1 MeV tritons (pink) and confined  
 201 tritons in  $B_t$  of 2.85 T (red), 2.75 T (blue), 2.65 T (green), 2.55 T (purple), and 1.375 T  
 202 (black) at  $R_{ax}$  of 3.60 m.



203

204 Figure 6. (a) The effect of  $R_{ax}$  on 1 MeV triton loss fraction. The loss fraction significantly

205 increases with the outward shift of  $R_{ax}$ . (b) Pitch angle distribution of launched 1 MeV

206 triton (pink) and confined tritons in  $B_t(T)/R_{ax}(m)$  of 3.55/2.79 (red), 3.60/2.75 (green),

207 3.75/2.64 (blue), and 3.90/2.54 (purple). Confinement of tritons having transition orbit is

208 significantly degraded with outward shift of  $R_{ax}$ .

209

#### 210 4. Summary

211 The study of the magnetic configuration effect on the first orbit loss of 1 MeV tritons is



212 performed using Lorentz orbit calculation code LORBIT. First orbit loss mainly appears  
213  $t$  of less than  $10^{-5}$  s. Those losses mainly occur in transition region and in helically trapped  
214 region. Toroidal and poloidal distribution of loss points of tritons shows that the loss  
215 points are accumulated in one side of the helical coil case. Most of the tritons are confined  
216 in the normal toroidal magnetic field strength ( $B_t > 2.5$  T) condition in  $R_{ax}$  of 3.6 m. It is  
217 shown that the effect of  $B_t$  on first orbit loss is weak. In the half toroidal magnetic field  
218 strength condition ( $B_t = 1.375$  T), most of the tritons are lost and the result is consistent  
219 with the low triton burnup ratio obtained in experiments. The first orbit loss fraction is  
220 evaluated in the magnetic configurations where triton burnup experiments were  
221 performed. The loss fraction of tritons drops from 20% to 5% with the inward shift of  $R_{ax}$ .  
222 It is found that the first orbit loss fraction of transition and helically trapped 1 MeV tritons  
223 is significantly decreased with the inward shift of  $R_{ax}$ .

224

## 225 **Acknowledgments**

226 This work is supported partly by LHD project budgets (ULHH003 and ULHH034).

227

## 228 **References**

229 [1] Fasoli A *et al* 2007 *Nucl. Fusion* **47** S264

- 230 [2] Heidbrink W W and Sadler G J 1994 *Nucl. Fusion* **34** 535
- 231 [3] Barnes C W *et al* 1998 *Nucl. Fusion* **38** 597
- 232 [4] Heidbrink W W *et al* 1983 *Nucl. Fusion* **23** 917
- 233 [5] Hoek M *et al* IPP-Report IPP-1/320 1999
- 234 [6] Duong H H *et al* 1993 *Nucl. Fusion* **33** 211
- 235 [7] Nishitani T *et al* 1996 *Plasma Phys. Control. Fusion* **38** 355
- 236 [8] Jo J *et al* 2016 *Rev. Sci. Instrum* **87** 11D828
- 237 [9] Gori S *et al* 2001 *Plasma Phys. Controlled Fusion* **43** 137
- 238 [10] Okamura S *et al* 2000 *J. Plasma Fusion Res.* **3** 73
- 239 [11] Osakabe M *et al* 2017 *Fusion Sci. Technol.* **72** 199
- 240 [12] Isobe M *et al* 2018 *Nucl. Fusion* **58** 082004
- 241 [13] Wesson J 2004 *Tokamaks* 3rd ed (Oxford: Oxford University Press)
- 242 [14] Fujii K *et al* 2015 *Nucl. Fusion* **55** 063029
- 243 [15] Ito R *et al* 1993 Analytic cross sections for collisions of H, H<sub>2</sub>, He and Li atoms and
- 244 ions with atoms and molecules JAERI-M 93-117 Japan: Japan Atomic Energy Research
- 245 Institute
- 246 [16] Isobe M, Funaki D and Sasao M 2009 *J. Plasma Fusion Res.* **8** 330
- 247 [17] Murakami S 2004 *J. Plasma Fusion Res.* **80** 725 (in Japanese)

248 [18] Homma M *et al* 2015 *Plasma Fusion Res.* **10** 3403050

249